23rd ABCM International Congress of Mechanical Engineering
December 6-11, 2015, Rio de Janeiro, RJ, Brazil

PERFORMANCE OF A MULTIGRID ALGORITHM APPLIED TO POISSON EQUATION WITH ADDITIONAL DATA WITHIN THE DOMAIN OF THE TYPE "SMALL ISLANDS"

Réverton Luis Antunes Neundorf
Meteorological System of Paraná State SIMEPAR, Curitiba/PR, Brazil
reverton@simepar.br

Leonardo Calvetti
Meteorological System of Paraná State SIMEPAR, Curitiba/PR, Brazil
leonardo@simepar.br

Marcio Augusto Villela Pinto
Federal University of Paraná, Department of Mechanical Engineering, Curitiba-PR, Brazil
marcio_villela@ufpr.br

Luciano Kiyoshi Araki
Federal University of Paraná, Department of Mechanical Engineering, Curitiba-PR, Brazil
lucaraki@ufpr.br

Abstract. *This work aimed to study a methodology that integrates rainfall estimates gathered by satellite, radar and rain gauge measurements by solving numerically a Poisson equation. It has been found that by introducing rain gauge measurements as additional conditions on the domain, which is a requirement of this methodology, the multigrid method does not converge, a problem associated with small-scale singularities that are invisible on coarser grids, such as "small islands". In order to study this problem, we used the finite difference method (FDM) and a second-order accuracy Central Differencing Scheme (CDS) for the discretization of mathematical models. Gauss-Seidel method was used as solver. For all studied cases, numerical solutions were obtained by applying geometric multigrid method (GMG) with the following characteristics: correction scheme (CS), full-weighted restriction operator, prolongation by bilinear interpolation and the use of the maximum number of levels. The "small islands" problem was solved by imposing additional conditions on the domain, in an appropriate way, in all meshes used by the multigrid method. The results are considered positive because the multigrid method converges to the numerical solution of Poisson's Equation.*

Keywords: *multigrid, iterative methods, finite difference method, small islands*

1. INTRODUCTION

In this work, we studied a methodology that integrates rainfall estimates gathered by satellite, radar and rain gauge measurements. Data blending technique was developed by Reynolds (1988) for temperature, and adapted by Xie and Arkin (1996) for rainfall, and it was used to integrate satellite rainfall estimates with rain gauge data. Vila *et al.* (2009), also used the methodology of Xie and Arkin (1996) to integrate satellite estimates with rain gauge measurements.

The methodology for blending rain estimates from Xie and Arkin (1996) basically consists in solving a Poisson equation with Dirichlet boundary conditions and source term given by the satellite, as well as enriching the domain with rainfall data measured by rain gauges. We adapted this methodology to integrate satellite estimates, as performed by Xie and Arkin (1996) and Vila *et al.* (2009), as well as radar estimates. For execution purposes, it is required:

1) Application of the methodology every 1 hour (in the future, 15 minutes).
2) Support for an arbitrary number of rain gauges, radars and satellites.
3) Solution of a Poisson equation for each radar and satellite involved in the integration.
4) Grid resolution of up to 4097×4097 points (also called mesh elements or pixels in the context of radars and satellites).
5) Regular and uniform grids (in all directions).

Thus, the need of a numerical method capable of solving Poisson's Equation within the operational interval of currently one hour is evident.

The discretization process of the domain and of the differential equations of the mathematical model, in this work, Poisson's equation, results in a system of equations of the kind, $A\mathbf{u} = \mathbf{b}$, where *A* is the coefficients matrix, $\mathbf{b}$ is the independent terms vector and $\mathbf{u}$ the unknowns vector.

Many computational techniques are studied aimed at solving the system $A\mathbf{u} = \mathbf{b}$ with the lowest computational cost (CPU time) and the closest solution to the analytical solution. Small linear systems (of the size of 10^2 elements) are solved fairly well by direct methods, such as Gauss elimination, but in practical applications they are not recommended due to the high inversion cost of the *A* matrix (Golub and Van Loan, 1989). For large linear systems, iterative methods are more suitable (Burden and Faires, 2008), since they have computational cost of the order of $O(N^2/2)$, considerably lower than the cost of the order of $O(N^3)$ of the direct methods, where *N* is the number of the unknowns.

The multigrid method belongs to the family of iterative methods used to solve efficiently partial differential equations and aims to accelerate the convergence of the iterative method in which it is applied (Tannehill *et al.*, 1997).

Multigrid methods are one of the most effective techniques used in the solution of elliptic equations, such as Poisson's equation (Briggs *et al.*, 2000; Trottenberg *et al.*, 2001), because the number of arithmetic operations that must be performed to achieve the discretization error level is proportional to the number of unknowns of the system of equations to be solved.

2. BLENDING METHODOLOGY

The methodology of Reynolds (1988), adapted by Xie and Arkin (1996) to the context of rainfall, integrates satellite estimates (and radar in this work) and rain gauge measurements by assuming that the spatial distribution, or the "shape" of the blended analysis, *B*, satisfies Poisson's equation

$$\nabla^2 B = f \tag{1}$$

where the source term f in Eq. (1) is determined with

$$f = \nabla^2 F \tag{2}$$

in which *F* represents radar or satellite estimates. In pixels where rain gauge measurements are available, the value of field *B* is equaled to the value of the rain gauges.

If rain gauge measurements are not available in the same pixels, the boundary conditions are given by the values of *F*.

The blending algorithm consists in:

1) Calculating the source term, Eq. (2), for each radar and satellite involved in the blending.
2) Equating *B* field values for each pixel that contains data measured by rain gauges.
3) Solve numerically Eq. (1) for each member (radars and satellites) using the calculated field *B* as initial guess for the next member considered.

Fig. 1 shows the area for which Eq. (1) is being solved. The circles represent the area covered by four S-Band Weather Radars, two from IPMet/Unesp in São Paulo State and two from Simepar in Paraná State. The red lines represent the territorial boundary of the states of Mato Grosso do Sul, São Paulo, Paraná and Santa Catarina whereas the black dots represent the distribution of rain gauges available for study.

3. MATHEMATICAL AND NUMERICAL MODELS

The domain discretization, each radar (circle) shown in the Fig.1 as well as the intersection area of all radars, was performed using uniform grids in all directions (latitude and longitude). For each pixel (or grid point) on the grid, Eqs. (1) and (2) were discretized with the finite difference method (FDM) employing central difference scheme (CDS), which consists in replacing the Laplacian of Eqs. (1) and (2) by algebraic expressions of the form

$$\nabla^2 \phi = \frac{\partial^2 \phi}{\partial lat^2} + \frac{\partial^2 \phi}{\partial lon^2} = \frac{\phi_{i+1,j} - 2\phi_{i,j} + \phi_{i-1,j}}{h_{lon}^2} + \frac{\phi_{i,j+1} - 2\phi_{i,j} + \phi_{i,j-1}}{h_{lat}^2} \tag{3}$$

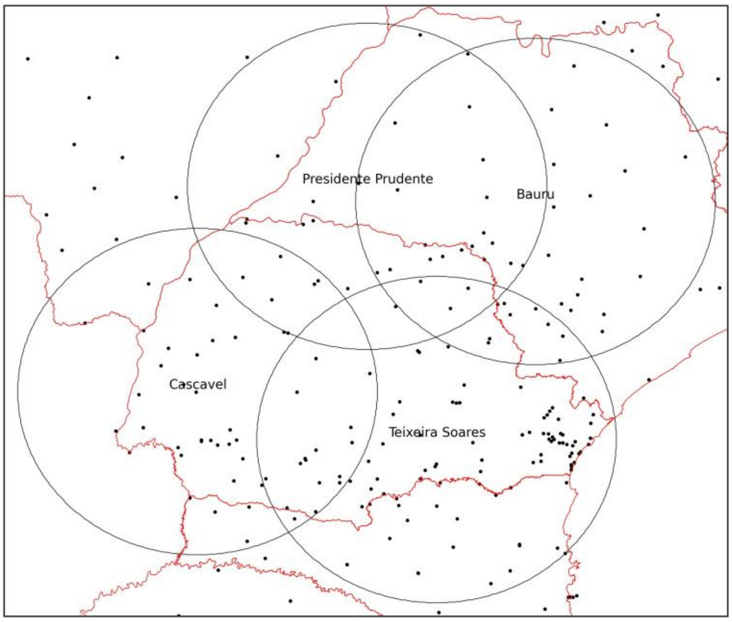

Figure 1. Area of study

where *lat* and *lon* represent the geographic coordinates of latitude and longitude, respectively. The variable ϕ represents *B* or *F* and in which $h_{lon} = h_{lat} = h$ was used. Replacing the Eq. (3) in the Eq. (1)

$$-4B_{i,j} + B_{i-1,j} + B_{i+1,j} + B_{i,j-1} + B_{i,j+1} = h^2 f_{i,j} \tag{4}$$

The source term $f_{i,j}$ must be previously obtained with

$$f_{i,j} = \frac{-4F_{i,j} + F_{i+1,j} + F_{i-1,j} + F_{i,j+1} + F_{i,j-1}}{h^2} \tag{5}$$

The Eq. (4) results in a linear system of the kind $A\mathbf{u} = \mathbf{b}$ that will be solved with the geometric multigrid method whose main feature is to employ a hierarchy of grids aiming to accelerate the convergence of the numerical solution.

The main idea of the multigrid method consists in applying recursively the two-grid correction scheme:

a) Smooth $A^h\mathbf{u}^h = \mathbf{b}^h$ (with an iterative method) to obtain $\mathbf{v}^h$ (an approximation of $\mathbf{u}^h$);
b) Compute the residual with $\mathbf{r}^h = \mathbf{b}^h - A^h\mathbf{v}^h$;
c) Transfer (restrict) the residual $\mathbf{r}^h$ to the coarser grid to obtain $\mathbf{r}^H$;
d) Smooth $A^H\mathbf{e}^H = \mathbf{r}^H$ (residual equation) to obtain $\mathbf{e}^H$;
e) Transfer (interpolate) the error $\mathbf{e}^H$ back to the finer grid to obtain $\mathbf{e}^h$;
f) Using the definition of error correct $\mathbf{u}^h$ with $\mathbf{u}^h = \mathbf{v}^h + \mathbf{e}^h$.

The superscripts *h* and *H* have been used to indicate, respectively, the fine and coarse grids on which the vectors are defined.

In order to increase the multigrid method performance, many grid levels must be used (Tannehill *et al.*, 1997). Pinto and Marchi (2007) as well as Oliveira (2010) suggest using all available levels. The order in which the grids are visited is called multigrid cycle. There are many types of multigrid cycles such as V-Cycle, W-Cycle, among others (Briggs *et al.*, 2000; Trottenberg *et al.*, 2001). We used exclusively V-Cycle, since W-Cycle is 50% more expensive regarding the number of operations involved (Hirsch, 1988). Fig.2 shows an example of a V-Cycle.

3.1 Multigrid details and test case

Eq. (4) is solved with geometric multigrid method with the following characteristics: correction scheme (CS), full-weighted restriction operator, prolongation by bilinear interpolation, use of the maximum number of levels and

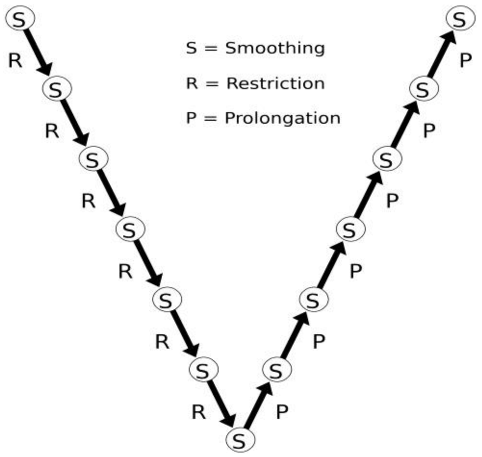

Figure 2. V-Cycle

standard coarsening ratio $r = 2$ (Briggs *et al.*, 2000; Trottenberg *et al.*, 2001). Gauss-Seidel method was used as solver. Three smoothing steps were performed on both pre-smoothing (before the residual restriction) and post-smoothing (after the interpolation of the error) (Oliveira, 2010). The stopping criteria used to interrupt the iterative process is the l_2-norm of the residual divided by the l_2-norm of the residual in the initial guess (Briggs *et al.*, 2000; Trottenberg *et al.*, 2001) represented by $\| \mathbf{r}_n \|_2 / \| \mathbf{r}_0 \|_2$ as it is less than 10^{-10}. In all the simulations, the multigrid method departed from the finest mesh and went towards the coarsest mesh possible (Pinto and Marchi, 2007; Oliveira, 2010).

In order to verify the validity of the implemented multigrid method, a two-dimensional heat conduction problem governed by the following differential equation was solved:

$$\frac{\partial^2 T}{\partial x^2} + \frac{\partial^2 T}{\partial y^2} = -2\Big[(1-6x^2)y^2(1-y^2) + (1-6y^2)\,x^2(1-x^2)\Big] \tag{6}$$

where *x* and *y* are the coordinate directions and *T* is the temperature. The boundary conditions of Dirichlet are given by

$$\begin{aligned} T(0,y) &= T(x,0) = 0 \\ T(1,y) &= T(x,1) = 0 \end{aligned} \tag{7}$$

such as the analytical solution of Eq. (6) is given by (Oliveira, 2000)

$$T\;\; x,y\;\; = (x^2 - x^4)(y^4 - y^2) \tag{8}$$

3.2 The "small islands" problem

It has been found that by introducing rain gauge measurements as additional conditions on the domain, which is a requirement of the studied methodology, the multigrid method does not converge, a problem associated with small-scale singularities that are invisible on coarser grids, such as "small islands" (Brandt, 1998).

Similarly to the problem of "small islands", cases in which the domain presents "holes" are observed in cosmological simulations (Teyssier, 2002). In these cases, grid coarsening results in a situation in which the boundary conditions on the domain cannot be represented in coarser grids (Guillet and Teyssier, 2011).

Brandt (1998) suggests as a possible solution to the "small islands" problem:

a) Enlarging the singularity on the coarser grid.
b) Modifying the interior coarse-grid equation near the singularity.
c) Recombining iterants. If the coarse grid equations are not modified, the convergence is slow, but only for a few very special components. Thus, slowness can be eliminated by recombining iterants (Brandt and Mikulinsky, 1995).

Johanse and Colella (1998) suggest stopping the residual restriction process when the "small islands" problem begins to affect the convergence of the multigrid.

McCorquodale *et al*. (2001), suggest modifying the Laplacian in the coarse grid so that the singularities are properly considered.

We used a methodology to solve the "small islands" problem that consists in applying step 2) of the blending algorithm in step d) of the two-grid correction scheme: for each solved residual equation $A\mathbf{e} = \mathbf{r}$ we verified if there are "near" rain gauges ("near" means "inside" of the grid element), and if so, the value of the pixel $\mathbf{e}_{i,j}$ is nulled.

4. RESULTS

Fig. 3 shows the l_2-norm of the residual in the nth V-Cycle divided by the l_2-norm in the initial guess, $\| \mathbf{r}_n \|_2 / \| \mathbf{r}_0 \|_2$, for the operational cases without proper treatment of the "small islands" problem. The disposition of the “small islands” in the domain can be observed in the Fig. 1 represented by the black dots.

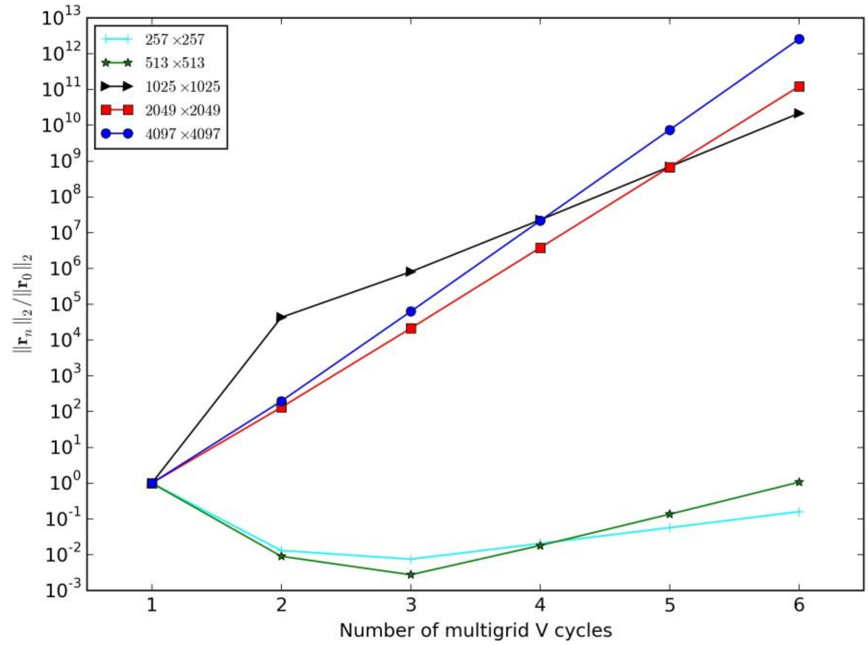

Figure 3. Increase in the residual for cases with “small islands”

Fig. 3 shows that the multigrid method does not converge due to the presence of "small islands". In order to verify the validity of the multigrid method, the implemented program was applied to the test case described in section 3.1. Fig. 4 (a) depicts the results.

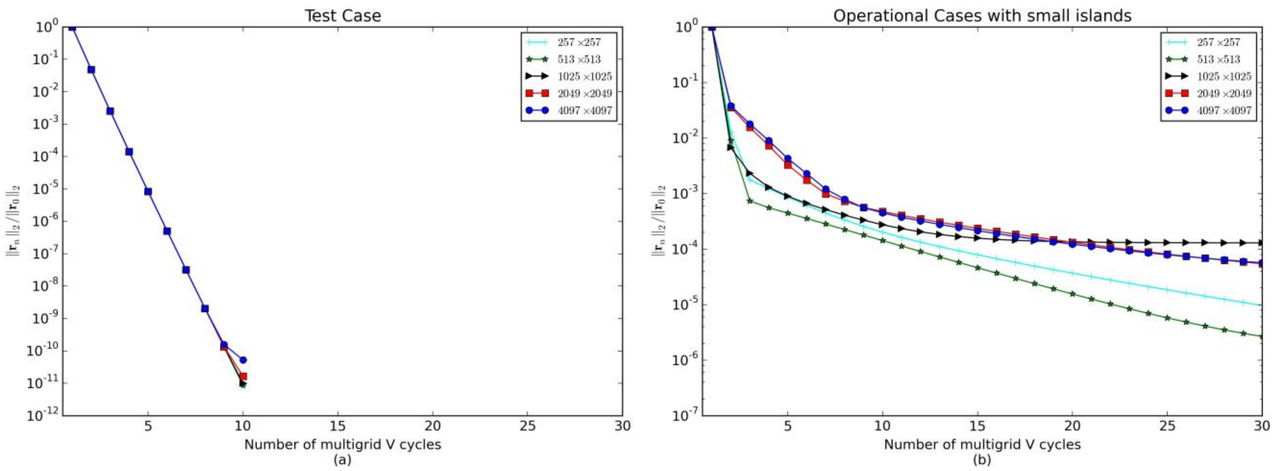

Figure 4. Decrease in the residual for test case (a) and operational cases (b) with “small islands”

Fig. 4 (a) shows that the implemented multigrid method presents fast convergence and achieves the specified tolerance, 10^{-10}, in just a few cycles; furthermore, results are presented for grids of sizes that vary from 257×257 to 4097×4097 pixels. One can notice that the convergence rate of the multigrid method, for this ideal case, does not depend on the size of the grid. After the iterative process, $\| \mathbf{r}_n \|_2 / \| \mathbf{r}_0 \|_2 \leq 10^{-10}$, the biggest absolute difference, in the whole domain, between the numerical and analytical solution was computed to be less than 3×10^{-9}.

Fig 4. (b) presents the results of the convergence of the multigrid method for the operational cases with the treatment of the "small islands" problems described in the section 3.2. Since there is no analytical solution for these cases, the numerical solution of the multigrid method was compared with the solution obtained with Gauss-Seidel method. As it can be seen in Fig. 4 (b), the convergence of the multigrid method showed dependence on the size of the problem, a phenomenon also observed by Guillet and Teyssier (2011), Day *et al*. (1998) and Popinet (2003).

Notice that some of the "small islands" shown in Fig. 1 may be unavailable and/or new "small islands" can be added during the initial processing of the rain gauge data. If the arrangement of "small islands" shown in Fig. 1 is changed, the convergence of the multigrid method (with the treatment described in the section 3.2) may be different from the results presented in Figure 4 (b).

Considering the methodology described in section 3.2, it is expected that the multigrid method exhibits convergence: a) ideal (Fig. 4 (a)) in case of non available rain gauges b) equal to the convergence of the used solver (Gauss-Seidel) in cases in which each grid element has a near rain gauge ($\mathbf{e} = 0$ for all the residual equations, which implies that additional grids are not used).

As a result of the methodology presented in section 3.2, we expect some of the coarser grids not be used ($\mathbf{e} = 0$ for the residual equation) in the correction process. If this happens, the multigrid method will not be using all the available grid levels. Fig. 5 shows the decrease in the residual for the test case with a 4097×4097 pixel grid and for the multigrid method using different numbers of grid levels.

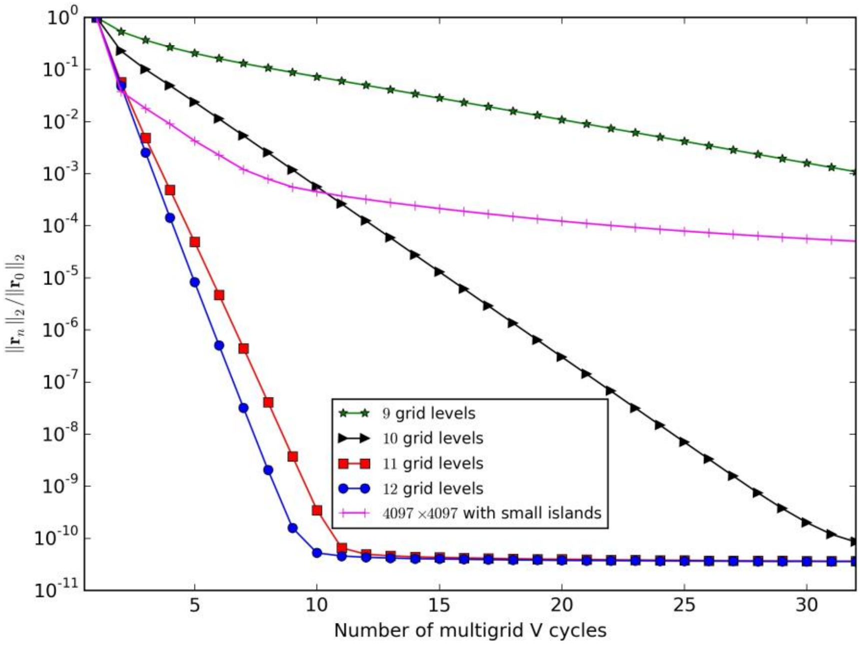

Figure 5. Decrease in the residual for different grid levels for the test case with $N = 4097 \times 4097$

Fig. 5 shows the importance (fastest decrease in the residual) of using all the available grid levels (12 for the standard coarsening of a grid with 4097×4097 pixels) and that, when less grid levels are used, more multigrid V cycles are needed to achieve the specified tolerance (10^{-10}).

Notice in Fig. 5 that by introducing rain gauge measurements as additional conditions on the domain and applying the treatment described in section 3.2, the convergence of the multigrid method is affected in a complex way: the first 4 V cycles show the fast convergence expected from the use of all the available grid levels, but the convergence slows down on the following V cycles. It could be said that after 10 V cycles, grid levels 10, 11 and 12 stop to contribute to the numerical solution of the problem.

Fig. 6 depicts the accumulated rainfall during 24 hours on June 14, 2015 as well as the rainfall estimates gathered by radar and satellite. The scale of Fig. 6 is 0-100 mm / 24h. For comparison reasons, the rainfall measured by rain gauges was interpolated using natural neighbor algorithm (natgrid) for the study area (Fig. 1).

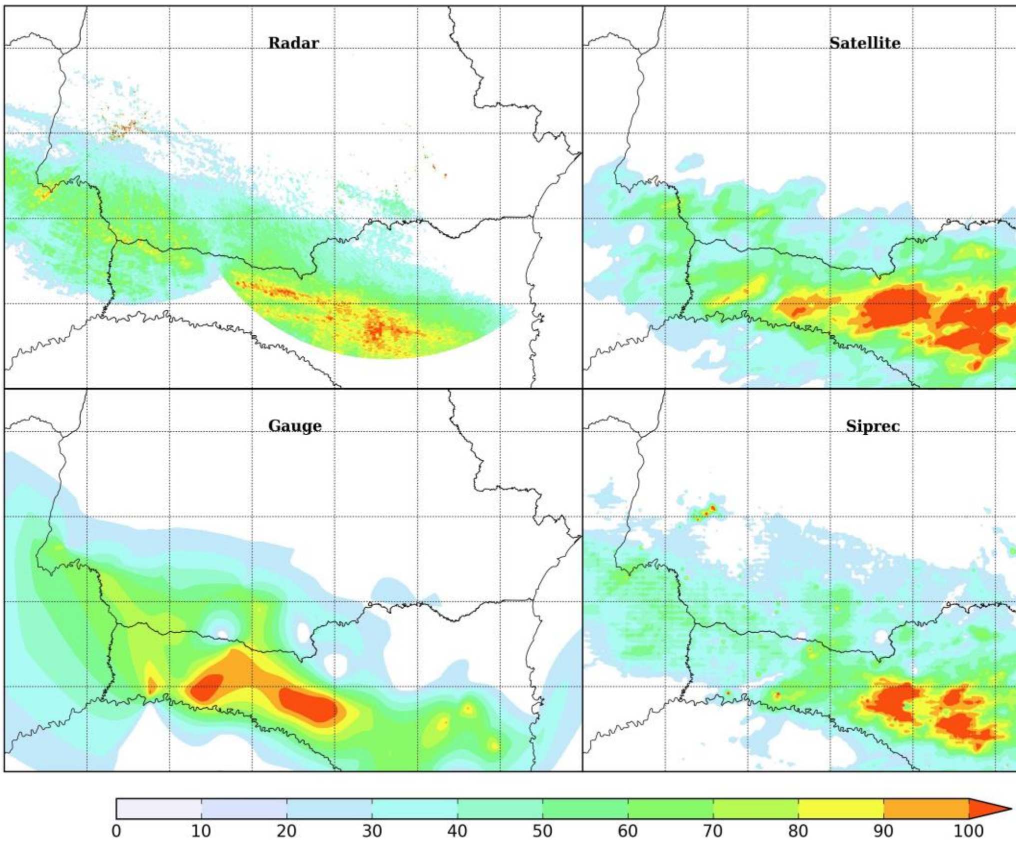

Figure 6. Map of rainfall (in mm/24h)

In Fig. 6, Siprec refers to the rainfall field resulting from the application of the Blending Methodology discussed in Section 2. The Siprec rainfall field characteristics will be discussed in a future work.

Although being only for illustrative purposes, Fig. 6 presents some of the challenges associated with blending radar, satellite and rain gauge data: radar and satellite have spatial representation but account only for rainfall estimates and differ over the intensity and positioning of rainfall. Rain gauges have no spatial representation; however, they represent actual measurements of rainfall.

5. CONCLUSION

In this work, we studied a methodology used to integrate rainfall estimates gathered by satellite, radar and rain gauge measurements, in which the imposition of constraints on the domain results in the non-convergence of the standard multigrid method. A solution capable to restore partially the convergence was presented. The undesirable relation of dependency between the convergence of the method and the size of the used grid is being studied and will be addressed in a future work.

6. ACKNOWLEDGEMENTS

The authors would like to thank the support of the Sistema Meteorológico do Paraná SIMEPAR and PPGMNE (Programa de Pós-Graduação em Métodos Numéricos em Engenharia).

7. REFERENCES

Briggs, W.L., Henson, V.E. and McCormick, S.F., 2000. *A Multigrid Tutorial.* SIAM, Philadelphia, 2nd edition.

Brandt, A. and Mikulinsky, V., 1995. "On recombining iterants in multigrid algorithms and problems with small islands". *SIAM Journal of Scientific Computing*, Vol. 16, p. 20-28.

Brandt, A., 1998. "Barriers to Achieving Textbook Multigrid Efficiency in CFD". ICASE Interim Report No. 32, NASA/CR-1998-207647. Appears as Appendix C in the textbook Multigrid, by U. Trottenberg, C.W. Oosterlee and A. Schuller, Academic Press, London, 2000.

Burden, R. L. and Faires, J. D., 2008. *Análise Numérica.* Tradutor: Ricardo Lenzi Tombi. São Paulo: Pioneira Thomson

Learning.

Day, M. S., Colella, P., Lijewski, M. J., Rendleman, C. A. and Marcus, D. L., 1998. “Embedded boundary algorithms for solving the Poisson equation on complex domains”. *Tech. Rep. LBNL-41811,* Lawrence Berkeley National Laboratory.

Golub, G. H. and Van Loan, C., 1989. *Matrix Computations*. Johns Hopkins Press, Baltimore, 2nd edition.

Guillet, T., and Teyssier, R., 2011. “A simple multigrid scheme for soving the Poisson equation with arbitrary domain boundaries”. *Journal of Computational Physics.* Vol. 230, p. 47-56.

Hirsch, C., 1988. *Numerical Computational of Internal and External Flows*. New York: John Wiley & Sons.

Johansen, H. and Colella, P., 1998. “A cartesian grid embedded boundary method for Poisson’s equation on irregular Domains”. *Journal of Computational Physics*. Vol. 147 (1), p. 60–85.

McCorquodale, P., Colella, P. and Johansen, H., 2001. “A cartesian grid embedded boundary method for the heat equation on irregular domains”. *Journal of Computational Physics*. Vol. 173 (2), p. 620–635.

Oliveira, F., 2010. *Efeitos de malhas anisotrópicas bidimensionais sobre o desempenho do método Multigrid geométrico.* Tese (Doutorado em Engenharia Mecânica), Universidade Federal do Paraná, Curitiba, PR.

Pinto, M. A. V. and Marchi, C. H., 2007. “Optimum Parameters of a Geometric Multigrid for the Two-Dimensional Laplace’s Equation”, *Proceedings of COBEM*.

Popinet, S., 2003. “Gerris: a tree-based adaptive solver for the incompressible Euler equations in complex geometries”. *Journal of Computational Physics*. Vol. 190, p. 572–600.

Tannehill, J.C., Anderson, D.A. and Pletcher, R.H., 1997. *Computational Fluid Mechanics and Heat Transfer*, Taylor & Francis, Washington, 2nd edition.

Reynolds, R. W., 1988. “A real-time global sea surface temperature analysis”. *J. Climate*, Vol. 1, p. 75-86.

Teyssier, R., 2002. “Cosmological hydrodynamics with adaptive mesh refinement a new high resolution code called RAMSES”. A&A385, p. 337–364.

Trottenberg, U., Oosterlee, C. and Schüller, A., 2001. *Multigrid*, Academic Press, San Diego.

Vila, D. A., de Goncalves, L. G. G., Toll, D. L. and Rozante, J. R., 2009. “Statistical evaluation of combined daily gauge observations and rainfall satellite estimates over continental South America”. *J. Hydrometeor*, Vol. 10, p. 533-543.

Xie, P. and Arkin, P. A., 1996. “Analysis of global monthly precipitation using gauge observations, satellite estimates, and numerical model predictions”. *J. Climate*, Vol. 9, p. 840-858.

8. RESPONSIBILITY NOTICE

The authors are the only responsible for the printed material included in this paper.